ELSEVIER

Heat treatment and thermally induced crystallization of glass for glass ionomer cement

Y.W. Gu [a,b,*], Y.Q. Fu [b]

[a] Singapore Institute of Manufacturing Technology, 71 Nanyang Drive, Singapore 638075, Singapore
[b] School of Mechanical and Production Engineering, Nanyang Technological University, Nanyang Avenue, Singapore 639798, Singapore

Abstract

The effect of heat treatment on the glass component for glass ionomer cements (GICs) has been studied, with specific reference to the microstructure, crystallization and phase transformation. The thermal crystallization was characterized by means of scanning electron microscopy, differential scanning calorimetry and X-ray diffraction. Results showed that there was an increase in the particle size after heat treatment. The glass presented three crystallization peaks. The activation energies for crystallization obtained by different analytical methods, namely Kissinger's, Ozawa's and Yinnon's methods, were in good agreement and revealed the propensity of this glass composition to crystallize easily. The crystalline activation energies for the glass determined by Kissinger's method were 670 and 336 kJ/mol, respectively, associated with the first and second peaks. The calculated Avrami parameters based on the two peaks were 1.58 and 2.97, respectively. The heat treatment produced a final product of strontium fluoride phosphate ($Sr_5(PO_4)_3F$) and mullite ($Al_6Si_2O_{13}$).
© 2004 Published by Elsevier B.V.

1. Introduction

In the late 1970s the glass ionomer cements (GICs) were developed as an outgrowth from the research into dental silicate cements [1]. GICs are currently used for various dental applications including root canal treatment and restorations of teeth. They have a number of advantages over polymethylmethacrylate (PMMA) bone cements. These include their good adhesion property to teeth, less toxic effect to dental pulp, continuous release of fluoride, as well as their lack of exothermic polymerization [2,3]. The good adhesive property and fluoride release of GICs contribute to reduce the rate of secondary caries both in filled teeth and on the enamel surfaces of adjacent teeth [4,5].

GICs consist of an aluminofluorosilicate glass powder and an aqueous polyacrylic acid. They have been classified as acid–base reaction cements [6]. They set initially by reaction of liquid polyacid ionomer with the divalent cations (e.g. Ca^{2+}) released from the glass to form insoluble polysalt.

Aluminium carboxylate structures are formed subsequently as the complex anionic alumino ions gradually give up their metal atoms as relatively discrete entities. Finally, the diffusionally controlled crosslinking of the polymer matrix enhances the strength, stiffness and insolubility of the cements.

Heat treatment has been used to deactivate the glass and hence allow the surgeon time to manipulate the prosthesis [7]. It was also found that heat treatment of glass could lead to an increase in the mechanical properties of the cement and reduction of thermal stresses in the glass particles induced by the shock cooling of the glass melts [8]. Amorphous glass is generally thermodynamically metastable and it can transform into relatively stable crystalline phases which are thermodynamically more stable upon heat treatment at certain temperatures. Therefore, the crystallization mechanism of glass needs to be investigated. In this study, the effect of heat treatment at different temperatures on the glass powders was studied prior to its use in the cement. The morphology and the phase composition of glass powders, as well as the temperature and activation energy with respect to the phase changes after heat treatment were investigated.

* Corresponding author. Tel.: +65-67938519; fax: +65-67925362.
E-mail address: mywgu@ntu.edu.sg (Y.W. Gu).

2. Experimental methods

The aluminosilicate glass powders were GC Fuji IX GP of A2 shade (GC Corporation, Japan). Energy dispersive spectroscopy (EDX) analysis identifies peaks of Al, Sr, Si, P, F and O elements [9,10]. Powders were subjected to DSC measurement (Netzsch 404 C with TASC 414/3A controller). DSC is a sensitive technique for establishing thermal changes within glass using approximately 40–50 mg of fine powders. The protective atmosphere used was nitrogen with a flow rate of 150 ml/min. Samples were heated in DSC from room temperature to 1173 K under various heating and cooling rates of 5, 10, 15 and 20 K/min to obtain the crystallization peak temperature, T_p, and the onset temperature T_x. The exothermic peaks shifted with the variation of heating rate. Based on the data of peak shifts versus heating rates, the activation energy for the crystallization was calculated by Kissinger's, Ozawa's and Yinnon's methods [11]. Activation energy for crystallization is an important kinetic parameter which indicates the thermal stability of the amorphous phases.

The glass powders were subjected to heat treatment at 823, 973, 1023 and 1173 K for half an hour following the apparent DSC crystallization peaks. Heat treatment was performed in a Carbolite furnace with a heating rate of 10 K/min to replicate the DSC analysis. The microstructural characteristics of glass powders after heat treatment were studied using Cambridge 360 scanning electron microscope (SEM). The mean particle size of the powders after heat treatment was measured by a Laser Particle Sizer (Fritsch Analyssette 22, Laval Lab Inc., Quebec, Canada). XRD was carried out to identify the crystalline phases within the glass powders after heat treatment. Data were collected by a Philips MPD 1880 diffactometer using Cu Kα radiation at 40 kV and 30 mA.

3. Results and discussion

Fig. 1 shows the morphology of glass powders after heat treatment at different temperatures. The original powder has a mean particle size of about 8 μm [10]. After heat treatment, the particle size increases. The particle size of the powders is observed to increase with increasing heat treatment temperature. The mean particle sizes of the powders after heat treatment at 823, 973 and 1173 K are 11, 17 and 22 μm, respectively. The increase of the particle size after heat treatment is due to the particle agglomeration, coalescence and growth at high temperatures.

The DSC curves of the glass powders obtained at a heating/cooling rate of 15 K/min are shown in Fig. 2. In this

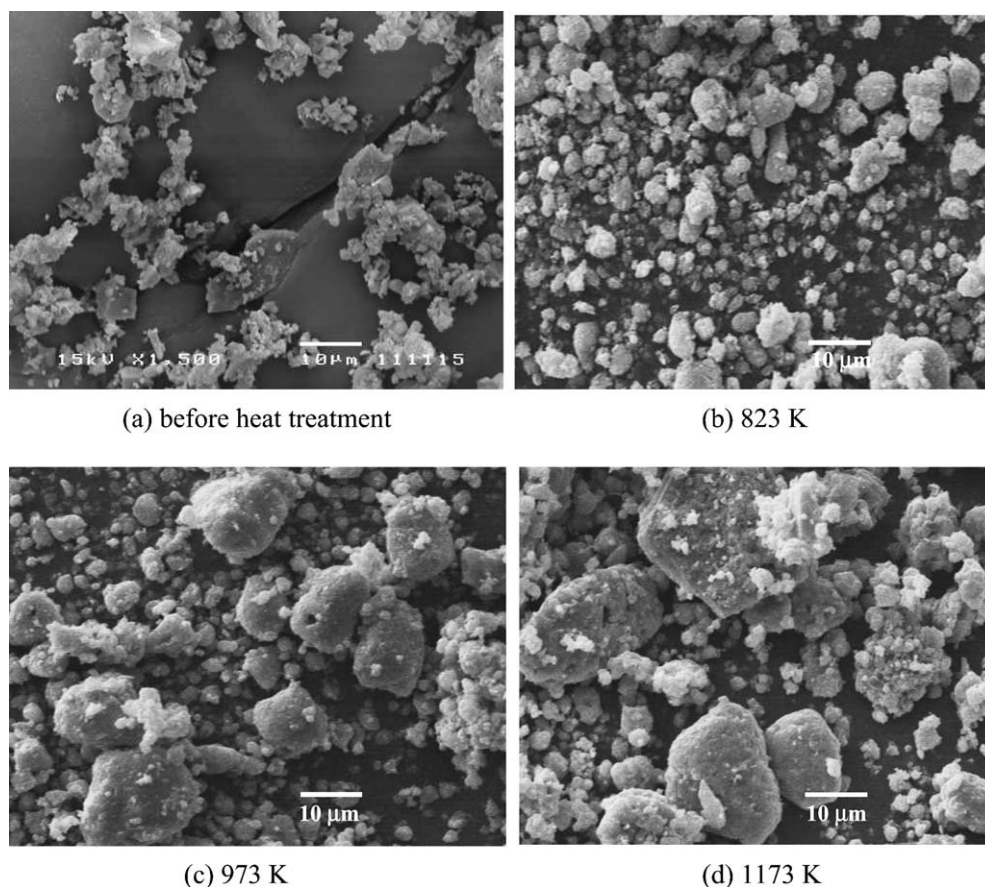(a) before heat treatment   (b) 823 K

(c) 973 K   (d) 1173 K

Fig. 1. Morphology of glass powders after heat treatment: (a) before heat treatment; (b) 823 K; (c) 973 K; (d) 1173 K.
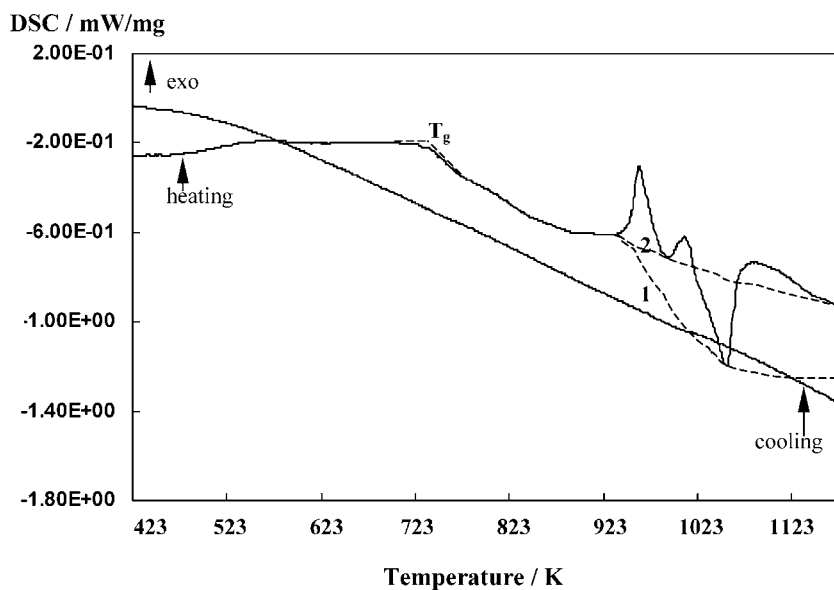
Fig. 2. DSC scan of glass powders (heating rate: 15 K/min).

figure, observed exothermic peaks are associated with crystallization process while T_g is the glass transition temperature. Based on Fig. 2, the glass powder presents $T_g = 729$ K. There are three crystallization peaks which occur immediately after each other in Fig. 2. The first peak presents the crystallization onset temperature (T_x) and peak temperature (T_p) of 951.5 and 959.5 K, respectively, while T_x and T_p values for the second peak are 1000.5 and 1008.5 K, respectively. The third peak shows a broad hump on the DSC curve and it is impossible to measure its peak temperature. Due to the loss of volatile silicon tetrafluoride (SiF$_4$) from the fine glass powders during the heating process, the glass transition temperature and crystallization temperatures may have been increased [12]. The presence of crystallization peaks indicates that there are exothermic chemical reactions going on during the temperature ranges of these peaks. The reaction product remains stable during cooling as no thermal effects can be observed during the cooling process (Fig. 2).

As can be observed in Fig. 2, there is a dip at 1038 K. It cannot be certain if the dip is an endotherm. For this reason, two possible baselines are suggested in Fig. 2. The crystallization onset temperature for the third peak is closely related to the selection of the baselines. If baseline path 2 is chosen, the onset temperature will be a higher temperature. If the dip at 1038 K is an endotherm, it is possible that a metastable intermediary phase has formed and it redissolves into the glass [13]. The endothermic event may also be attributed to the liquidus temperature of the residual glass [14]. In some traces, the baseline path 2 seems to indicate that the dip is simply the remainder of the first two peaks.

Fig. 3 shows the XRD patterns of glass powders after heat treatment. The glass powders before heat treatment shows that the structure of glass is a disordered and amorphous structure. The amorphous structure remains after heat treatment at 823 K. This is consistent with the DSC results, which indicates that there is no crystallization peak at the temperatures lower than 923 K. Crystallization takes place at the temperature above 973 K, as can be observed from Fig. 3. XRD results show the presence of strontium fluoride phosphate (Sr$_5$(PO$_4$)$_3$F) and mullite (Al$_6$Si$_2$O$_{13}$) after heat treatment. Mullite is formed as a second phase along with strontium fluoride phosphate [12]. Hill et al. reported that many calcium- and phosphate-containing ionomer-type glasses crystallized to calcium fluoride phosphate (Ca$_5$(PO$_4$)$_3$F) [12,15]. This is in consistent with the present investigation that strontium-containing glass crystallizes to strontium fluoride phosphate after heat treatment. The presence of strontium fluoride phosphate and mullite indicates that there is no significant loss of silicon tetrafluoride during heat treatment.

DSC crystallization peaks of the glass powders obtained at four heating rates ($V = 5$, 10, 15 and 20 K/min) are shown in Fig. 4. An increased rate of heating in the DSC machine produces a higher crystallization peak temperature and sharper peaks. The apparent activation energy for crystallization (E) can be determined by the variation of peak temperature (T_p) as a function of the heating rate (V). One of the commonly used methods was developed by Kissinger [1], showing a linear dependence between $\ln(T_p^2/V)$ and $1/T_p$:

$$\ln\left(\frac{T_p^2}{V}\right) = \frac{E}{RT} + C \tag{1}$$

where C is a constant and R is the universal constant. Ozawa proposed a different approach [16], which revealed that the plot of $\ln V$ versus $1/T_p$ was a straight line with a slope of E/R, as shown in Eq. (2). Yinnon and Uhlmann [17] suggested a method to obtain E by plotting $\ln(T_p/V)$ versus $1/T_p$, as
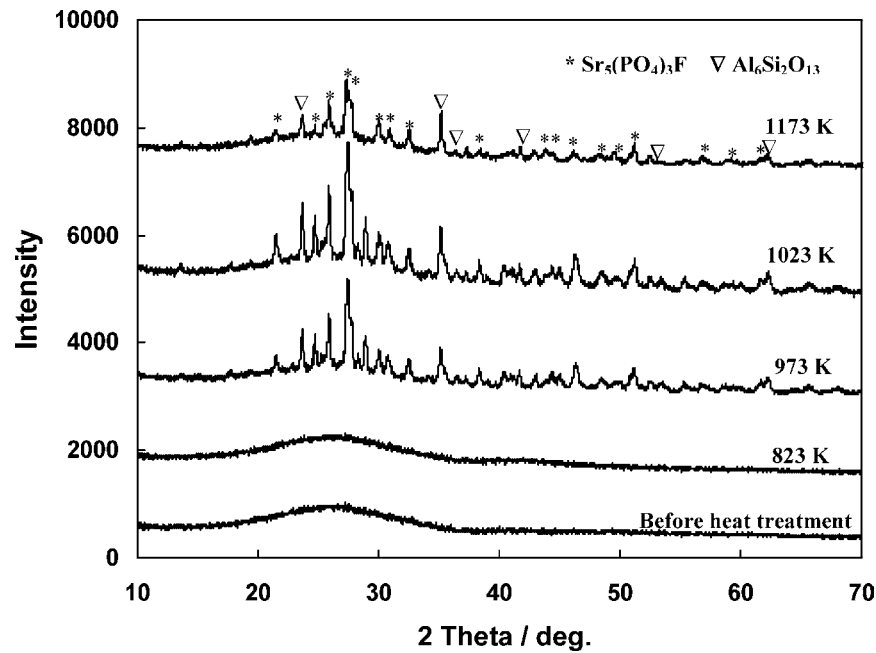
Fig. 3. XRD patterns of glass powders after heat treatment.

expressed in Eq. (3):

$$\ln V = \frac{E}{RT} + C \qquad (2)$$

$$\ln \left(\frac{T_p}{V} \right) = \frac{E}{RT} + C \qquad (3)$$

The third peak of the DSC curve obtained at a heating rate of 15 and 20 K/min is actually composed of two peaks, which can be observed from the DSC curves obtained at a lower heating rate of 5 K/min. Due to the overlapping of

the third and fourth crystallization peaks and the difficulties in the accurate measurement of the peak temperatures, the activation energies for the formation of the third and fourth peaks are not carried out. According to Eqs. (1)–(3), the plots of $\ln(T_p^2/V)$, $\ln(T_p/V)$ and $\ln V$ versus $1/T_p$ for the first and second crystallization peaks are shown in Fig. 5. A linear regression can be obtained and the activation energy can then be calculated from the slope of the straight lines. The calculated activation energies for the first peak obtained from Kissinger, Ozawa and Yinnon plots are 670, 684 and 652 kJ/mol, respectively. For the second peak, the activation
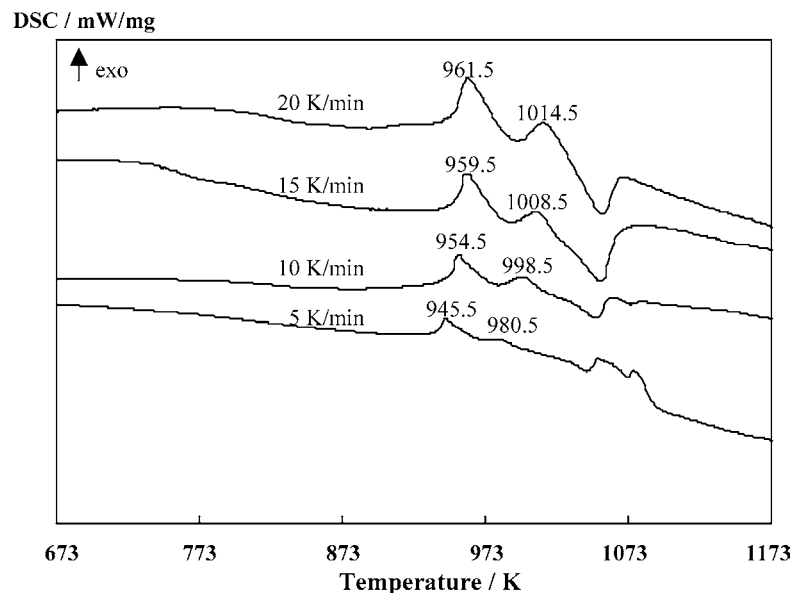

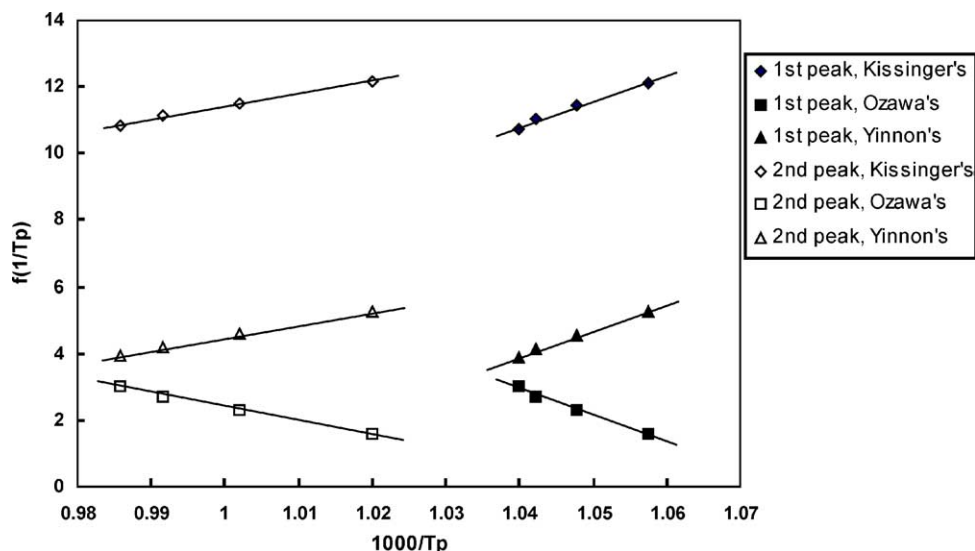Fig. 4. DSC curves with different heating rates.

Fig. 5. Kissinger, Ozawa and Yinnon plots for determining the activation energy of crystallization of glass powders.

energies of crystallization calculated from the three analytical methods are 336, 341 and 326 kJ/mol, respectively. The activation energies for crystallization of the first peak are greater than the activation energies of the second peak. The values of the activation energy obtained from the three analytical methods are in good agreement.

The Avrami exponent, *n*, is another important parameter which may be correlated to the crystallization mechanism. The Avrami parameter *n* can be expressed by the following equation [18]:

$$n = \left(\frac{2.5}{\Delta T}\right) \frac{RT_p^2}{E} \tag{4}$$

where ΔT is the width of the crystallization peak at half maximum.

The Avrami parameters of the first and second peaks of glass powders calculated from Eq. (4) are 1.58 and 2.97, respectively. According to Kissinger [19] and Reynoso [20], the first crystallization peak has a value of 1.58, which is probably associated with the surface crystallization.

From DSC and XRD results, it can be observed that the amorphous glass powders for glass ionomer cements can transform to crystalline phases easily upon heat treatment and this amorphous–crystalline transformation is probably associated with the surface crystallization. The presence of strontium fluoride phosphate and mullite indicates that these phases are easily formed, which may have consequently tied up a significant proportion of the strontium and aluminium in the glass and thus can delay the setting reaction of the cement when the glass powders are mixed with polyacrylic acid.

4. Conclusions

Crystallization mechanisms of glass powders were studied by DSC, XRD and SEM. The following conclusions can be made from this investigation:

(1) Crystallization of amorphous glass can be thermal induced. The crystallization gives rise to the formation of strontium fluoride phosphate ($Sr_5(PO_4)_3F$) and mullite ($Al_6Si_2O_{13}$).
(2) The activation energies for crystallization obtained by different analytical methods are in good agreement and reveal the propensity of this glass composition to crystallize easily.
(3) The crystalline activation energies for the glass determined by Kissinger's method are 670 and 336 kJ/mol, respectively, associated with the first and second peaks.
(4) The particle size of glass powders increases with increasing heat treatment temperature due to the particle agglomeration, coalescence and growth at high temperatures.

References

[1] A.D. Wilson, B.E. Kent, D. Clinton, R.P. Miller, J. Mater. Sci. 7 (1972) 220–238.
[2] I.M. Brook, P.V. Hatton, Biomaterials 19 (1998) 565–571.
[3] S.K. Sidhu, T.F. Watson, Am. J. Dent. 8 (1) (1995) 59–66.
[4] L. Forsten, Biomaterials 19 (1998) 503–508.
[5] S.G. Griffin, R.G. Hill, Biomaterials 21 (2000) 693–698.
[6] J.W. Nicholson, J.H. Braybrook, E.A. Wasson, J. Biomater. Sci. Polym. 2 (4) (1991) 277–285.
[7] A.D. Neve, V. Piddock, E.C. Combe, Clin. Mater. 12 (1993) 113–115.
[8] D. Wood, R. Hill, Biomaterials 12 (1991) 164–170.
[9] A. Stamboulis, R.V. Law, R.G. Hill, Biomaterials 25 (17) (2004) 3907–3913.
[10] Y.W. Gu, P. Cheang, A.U.J. Yap, R. Kumar, Biomaterials 25 (18) (2004) 4029–4035.
[11] H.E. Kissinger, Anal. Chem. 29 (1957) 1702.
[12] C.M. Gorman, R.G. Hill, Dent. Mater. 19 (2003) 320.

[13] K. Mackinnon, Effect of heat and chemical treatment on the structure of glass for glass-ionomer cements, Master's Thesis, Imperial College of Science, Technology and Medicine, 1998.

[14] A. Clifford, R.G. Hill, M.R. Towler, D.J. Wood, J. Mater. Sci. 36 (2001) 3955–3961.

[15] R.G. Hill, A. Stamboulis, R.V. Law, A. Clifford, M.R. Towler, C. Crowley, J. Non-Cryst. Solid 336 (2004) 223.

[16] T. Ozawa, Bull. Chem. Soc. Jpn. 38 (1965) 217.

[17] H. Yinnon, D.R. Uhlmann, J. Non-Cryst. Solids 54 (1983) 253.

[18] J.A. Augis, J.E. Bennett, J. Ther. Anal. 13 (1978) 283.

[19] H.E. Kissinger, J. Res. Bur. Stand. 57 (1956) 217.

[20] V.C.S. Reynoso, K. Yukimitu, T. Nagami, C.L. Carvalho, J.C.S. Moraes, E.B. Araujo, Mater. Lett. 56 (2002) 424–428.